Bull. Mater. Sci., Vol. 40, No. 1, February 2017, pp. 1–6. © Indian Academy of Sciences.
DOI 10.1007/s12034-016-1344-2

Synthesis and photoluminescence study of narrow-band UVB-emitting $LiSr_4(BO_3)_3:Gd^{3+}$, Pr^{3+} phosphor

A O CHAUHAN[1,*], N S BAJAJ[2] and S K OMANWAR[1]
[1]Sant Gadge Baba Amravati University, Amravati 444602, India
[2]Toshnival ACS College, Sengaon, Hingoli 431542, India

MS received 14 December 2015; accepted 27 May 2016

Abstract. **A series of Pr^{3+}, Gd^{3+} and Pr^{3+}–Gd^{3+}-doped inorganic borate phosphors $LiSr_4(BO_3)_3$ were successfully synthesized by a modified solid-state diffusion method. The crystal structures and the phase purities of samples were characterized by powder X-ray diffraction. Surface morphology of the sample was studied by scanning electronic microscopy (SEM). The optimal concentrations of dopant Gd^{3+} ions in compound $LiSr_4(BO_3)_3$ were determined through the measurements of photoluminescence (PL) spectra of phosphors. Gd^{3+}-doped phosphors $LiSr_4(BO_3)_3$ show strong band absorption in UV spectral region and narrow-band UVB emission under the excitation of 276 nm was only due to $^6P_J \rightarrow {}^8S_{7/2}$ transition of Gd^{3+} ions. The effect of Pr^{3+} ion on excitation of $LiSr_4(BO_3)_3:Gd^{3+}$ was also studied. The excitation of $LiSr_4(BO_3)_3:Gd^{3+}$, Pr^{3+} gives a broad-band spectra, which show very good overlap with the Hg 253.7 nm line. The photoluminescence spectra of $LiSr_4(BO_3)_3$ with different doping concentrations Pr^{3+} and keeping the concentration of Gd^{3+} constant at 0.03 mol have also been studied. The emission intensity of $LiSr_4(BO_3)_3:Pr^{3+}$–Gd^{3+} phosphors increases with increasing Pr^{3+} doping concentration and reaches a maximum at 0.01 mol. From the photoluminescence study of $LiSr_4(BO_3)_3:Gd^{3+}$, Pr^{3+} we conclude that there was efficient energy transfer from $Pr^{3+} \rightarrow Gd^{3+}$ ions in $LiSr_{4-x-y}Pr_xGd_y(BO_3)_3$ phosphors.**

Keywords. **Inorganic borate; SEM; photoluminescence; narrow-band UVB; energy transferred.**

1. Introduction

The spectrum of optical radiation (light) consists of different wavelengths of 'light' ranging from 100 nanometres (nm) in the ultraviolet (UV) range to 1 millimetre (mm) in the infrared (IR) range. A part of the whole electro-magnetic spectrum is occupied by ultraviolet radiation (UVR). The biological and physical characteristics permit convenient division of UVR into three parts such as UVC: the rays that do not pass through the earth's atmosphere (200–290 nm), UVB: the rays responsible for nearly all biological effects following sunlight exposure, including tanning, burning and skin cancer (290–320 nm) and UVA: those rays closest to the visible spectrum that pass through glass and are the least harmful to the skin (320–400 nm).

Ultraviolet B (UVB) has become the phototherapy treatment of choice for psoriasis, vitiligo, atopic dermatitis (eczema) and other photo-responsive skin disorders. UVB can be divided as narrow-band UVB and broadband UVB. Broadband UVB radiation has been used for the treatment of psoriasis for decades [1]. Various investigations imply that the most favourable range for the effective UVB treatment of psoriasis is in the long-wavelength part of the UVB spectrum, i.e., between 305 and 315 nm [2,3]. A narrow UVB source emitting at about 311 nm was made available around 1988 [4]. This has revolutionized the UVB phototherapy [2]. $LaB_3O_6:Gd^{3+}$, Bi^{3+} is a phosphor used in commercial narrow UVB phototherapy lamps. Sonekar *et al* [5] have reported borate host phosphor materials $LaBO_3$, LaB_3O_6, LaB_5O_9 and YBO_3 doped with Gd^{3+} ions for UV lamps.

The borate atom has two types of hybridized orbitals, the planar sp^2 and the three-dimensional sp^3, to coordinate three or four oxygen atoms to form various Bx–Oy complex anionic groups. Therefore many types of borate crystals have been found to be constructed based on these complex anionic groups [6]. Thus, inorganic borates have drawn lot of research because of their variety of structure types, transparency to a wide range of wavelengths, high laser damage tolerance and high optical quality. A variety of BO atomic groups are considered to be dominant for the physical properties, in particular the optical properties of borates.

However, to the best of our knowledge, although the luminescence properties of Ce^{3+}, Tb^{3+}, Eu^{3+}, Dy^{3+}, Eu^{2+}-doped $LiSr_4(BO_3)_3$ have been reported [7–11], photoluminescence properties of Gd^{3+}–Pr^{3+}-doped $LiSr_4(BO_3)_3$ have not yet been studied.

In the present work, pure, Gd^{3+}-doped $LiSr_4(BO_3)_3$ and Pr^{3+}–Gd^{3+}-doped $LiSr_4(BO_3)_3$ materials were prepared by a modified solid-state diffusion method. The phase purity of synthesized materials was characterized using powder X-ray diffraction (XRD). After synthesis and characterization

*Author for correspondence (abhi2718@gmail.com)

of the materials, the photoluminescence properties of the synthesized materials were studied using a spectrofluorometer at room temperature.

2. Experimental

The phosphors $LiSr_4(BO_3)_3$ doped with Pr^{3+}, Gd^{3+} and Gd^{3+}–Pr^{3+} were prepared by a modified solid-state diffusion method. Palan *et al* [12,13] and Bajaj *et al* [14] reported the modified solid-state diffusion method. Stoichiometric amounts of high-purity (Analytical Reagent) starting materials lithium nitrate ($LiNO_3$), strontium nitrate ($Sr(NO_3)_2$), boric acid (H_3BO_3) and stock solution of gadolinium nitrate ($Gd(NO_3)_3$) (99.99% purity) and praseodymium nitrate ($Pr(NO_3)_3$) (99.99% purity) were used for preparation of phosphors. Stoichiometric amounts of starting materials with a little amount of double distilled water were mixed thoroughly in a china basin to obtain a homogeneous solution. The solution was slowly heated at a low temperature of 90°C in order to remove the excess of water contents. The thick paste obtained after heating was then transferred into a microwave furnace maintained at 200°C for 1 h. After that the temperature of microwave furnace was increased up to 400°C and the material was kept for 1 h. Then the sample was grinded using a mortar and a pestle, placed in the microwave furnace maintained at temperature 900°C for 3 h and then quenched to room temperature. The resultant powder sample was then characterized using powder XRD and a spectrofluorometer. The complete process involved in the reaction is represented as a flow chart in figure 1.

3. Characterization of samples

The phase purities of $LiSr_4(BO_3)_3$:Gd^{3+} and $LiSr_4(BO_3)_3$:Gd^{3+}, Pr^{3+} samples were studied using a Rigaku miniflex II X-ray Diffractometer at a scan speed of 4° min^{-1} and CuKα ($\lambda = 1.5406$ Å) radiation in the range 10–70°. The photoluminescence excitation and emission spectra were measured at room temperature using a Hitachi F-7000 spectrofluorometer in the range 200–400 nm. The parameters such as spectral resolution, width of the monochromatic slits (1.0 nm), photomultiplier tube (PMT) detector voltage and scan speed were kept constant throughout the analysis of samples.

4. Results and discussion

4.1 *XRD of $LiSr_4(BO_3)_3$ phosphor*

The diffraction pattern is usually used to identify the crystal structure and the phase purity of the sample. Figure 2 displays the powder XRD patterns of polycrystalline $LiSr_4(BO_3)_3$:Gd^{3+} and $LiSr_4(BO_3)_3$:Gd^{3+}, Pr^{3+} samples prepared using the modified solid-state diffusion method. The XRD pattern for $LiSr_4(BO_3)_3$ agrees well with ICDD file no. 01-073-3772. The high-intensity peaks observed at 23.7862°, 34.8895°, 41.8262° and 54.8805° from the ICDD file show exact matching with the XRD pattern of material prepared by the modified solid-state diffusion method. This agreement indicates that the material $LiSr_4(BO_3)_3$ was successfully prepared using the modified solid-state diffusion method. The crystal structure of the prepared materials can

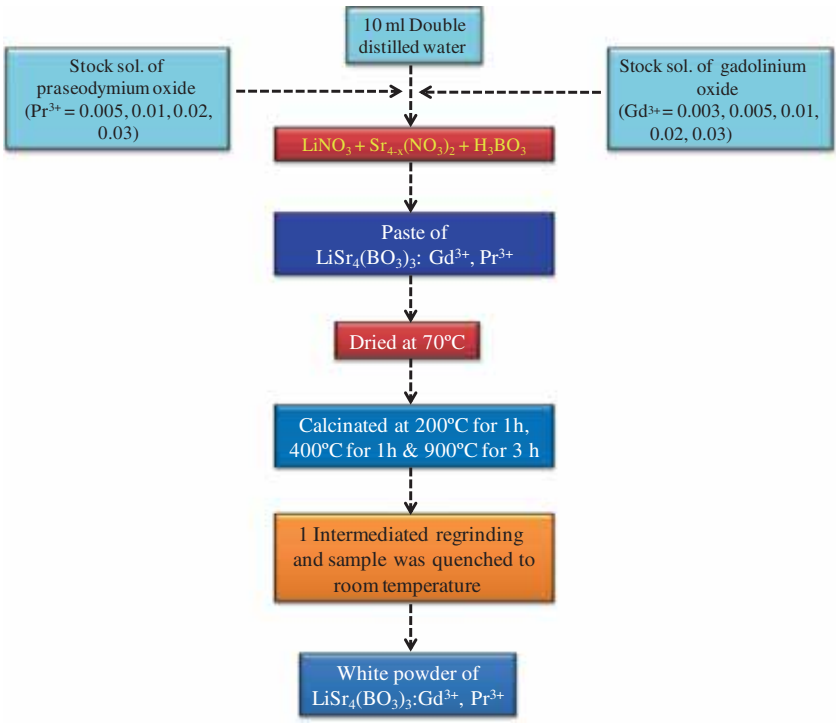

Figure 1. Flowchart of $LiSr_4(BO_3)_3$:Pr^{3+}, Gd^{3+} synthesis by solid-state diffusion method.

be refined to be cubic, with $a = b = c = 14.9509$ Å. The materials crystallize in the centro-symmetric space group Ia-3d (230). From figure 2 it is observed that the position and intensity of the main peak are the same. No impurity line is observed, indicating only crystalline product in the sample.

Considering the effective ionic radii of cations (Sr^{2+} = 131 pm, Pr^{3+} = 117.9 pm, Gd^{3+} = 110.7 pm for nine-fold coordination, and Pr^{3+} = 99 pm, Gd^{3+} = 93.8 pm for six-fold coordination), Pr^{3+} or Gd^{3+} ions are expected to enter Sr^{2+} sites in the host lattices [15]. The average crystalline size of $LiSr_{4-x-y}Gd_xPr_y(BO_3)_3$ phosphor was found to be 85.59 nm as estimated by Scherrer's formula

$$D = \frac{K\lambda}{\beta \cos\theta},$$

where θ is the Bragg angle of diffraction lines, K a shape factor taken as 0.90, λ the wavelength of incident X-rays (λ = 0.154 nm) and β the full-width at half-maximum (FWHM in radians).

4.2 *Morphology of $LiSr_4(BO_3)_3$*

In order to study topography of as-synthesized sample, FE-scanning electronic microscopy (SEM) analysis was done and the images are displayed in figure 3. The representative micrograph shows that the synthesized sample has irregular shape with agglomeration. The $LiSr_4(BO_3)_3$ prepared by the modified solid-state diffusion method yields agglomerated particles with cubic edges. The average size of as-synthesized phosphor particles is about 2–5 μm, which is appropriate for a phosphor.

4.3 *Photoluminescence spectra*

Figure 4 demonstrates the photoluminescence spectrum of $LiSr_4(BO_3)_3$:Pr^{3+}. The phosphor shows broad excitation band from 210 to 260 nm with a maximum at 245 nm. The phosphors give strong and a much broader emission spectrum from 260 to 370 nm having two shoulder peaks at 280 and 325 nm under the excitation of 245 nm. These obtained emission spectra show the parity allowed interconfigurational optical transition from $4f^15d^1$ (lowest excited level of Pr^{3+}) state to the ^3H_J and ^3F_J multiplets of ground $4f^2$ electronic configuration. Moreover the effect of concentration of Pr^{3+} has also been studied by preparing the $LiSr_4(BO_3)_3$:Pr^{3+} materials with assorted doping concentration of Pr^{3+} ions. It was observed that emission intensity of the phosphor increases gradually by increasing the concentration of dopant, i.e., Pr^{3+}. At the 0.01 mol concentration

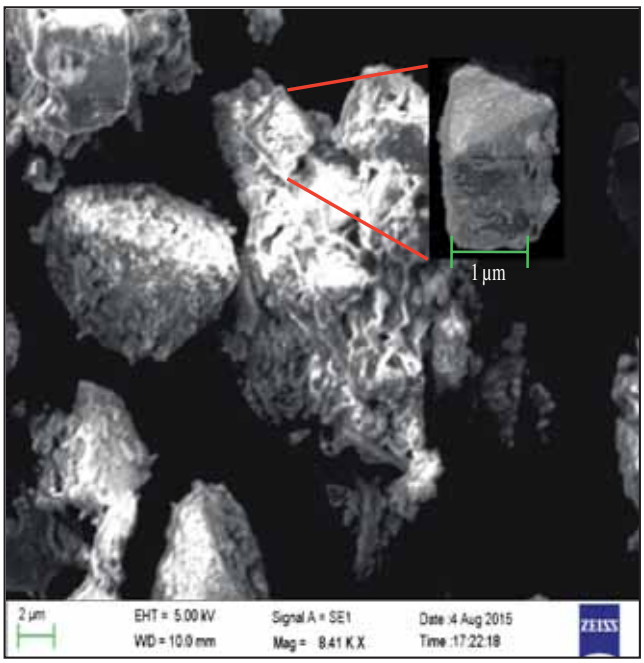

Figure 3. SEM image of the $LiSr_4(BO_3)_3$:Gd^{3+}, Pr^{3+} phosphor synthesized by solid-state diffusion method.

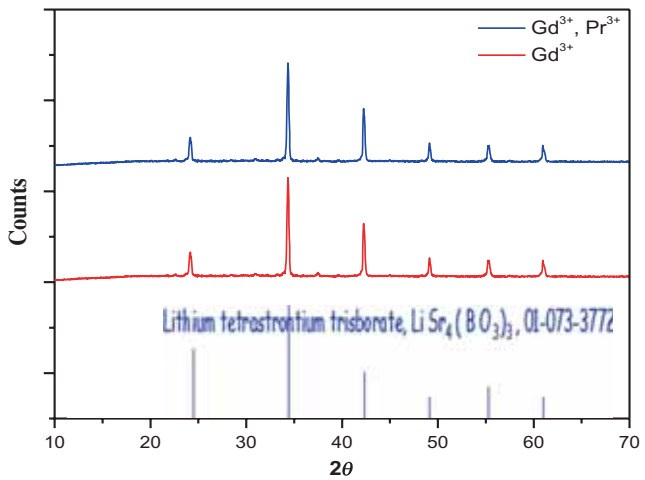

Figure 2. XRD patterns of the $LiSr_4(BO_3)_3$: Gd^{3+} and $LiSr_4(BO_3)_3$:Gd^{3+}, Pr^{3+} phosphor synthesized by solid-state diffusion method.

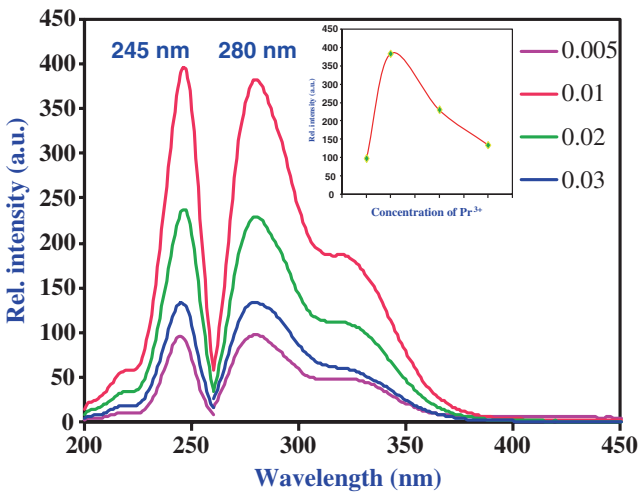

Figure 4. Combined excitation and emission spectra of $LiSr_{4-x}(BO_3)_3$:xPr^{3+} (x = 0.005, 0.01, 0.02 and 0.03).

of Pr^{3+}, the phosphor possesses maximum emission intensity. As the doping concentration of phosphor goes beyond the 0.01 mol the emission intensity of the synthesized phosphor suddenly decreases due to the well-known phenomenon of concentration quenching (shown in the inset of figure 4).

According to Blasse [16], in the luminescence, a phenomenon of energy transfer from one activator to another until all the energy is consumed is known as concentration quenching. The concentration quenching phenomena is observed because of non-radiative energy transfer among the identical ions. It is well recognized that the concentration quenching phenomena will not take place if the average distance between the identical ions is so large that the energy migration is weak. The critical distance is an essential parameter to understand the phenomenon, as the probability of energy transfer between two activators is inversely proportional to the n^{th} power of the distance of the activator ions. The critical distance R_C can be estimated using the following formula:

$$R_C \approx 2\left(\frac{3V}{4\pi\chi_c N}\right)^{1/3},$$

where V is the volume of the unit cell (in $Å^3$), χ_c is the atom fraction of activator at which the quenching occurs, the so-called optimum concentration and N is the number of cations in the unit cell. Crystallographic data for $LiSr_4(BO_3)_3:Pr^{3+}$ gives the value of $\chi_c = 0.01$, $N = 16$ and $V = 3341.805$ $Å^3$; thus the critical energy transfer distance R_C of $LiSr_4(BO_3)_3:Pr^{3+}$phosphor is calculated to be about 34.17 Å.

Figure 5 demonstrates combined emission and excitation spectra of $LiSr_{4-x}(BO_3)_3$ with varying concentration of Gd^{3+} (relative to Sr^{2+}) prepared by the modified solid-state diffusion method. The emission is in the form of a narrow band round 313 nm corresponding to $^6P_J \rightarrow {}^8S_{7/2}$ transition upon excitation with 276 nm. The emission spectra consist of a weak line at 306 nm followed by a strong one at 313 nm, which correspond to the $^6P_{5/2} \rightarrow {}^8S$ and $^6P_{7/2} \rightarrow {}^8S$ transitions of the Gd^{3+} ion, respectively. The concentration of Gd^{3+} (relative to Sr^{2+}) for which maximum intensity of emission is obtained was found to be 0.03 mol. The critical distance R_C of the energy transfer between the same activators Gd^{3+} in $LiSr_4(BO_3)_3:Gd^{3+}$ can be calculated using the above-mentioned formulae of critical distance. By taking the value of χ_c, V and N to be 0.03, 3341.805 $Å^3$ and 16, respectively, the critical distance was found to be 23.69 Å. The stokes shift was calculated to be 4283 cm^{-1}.

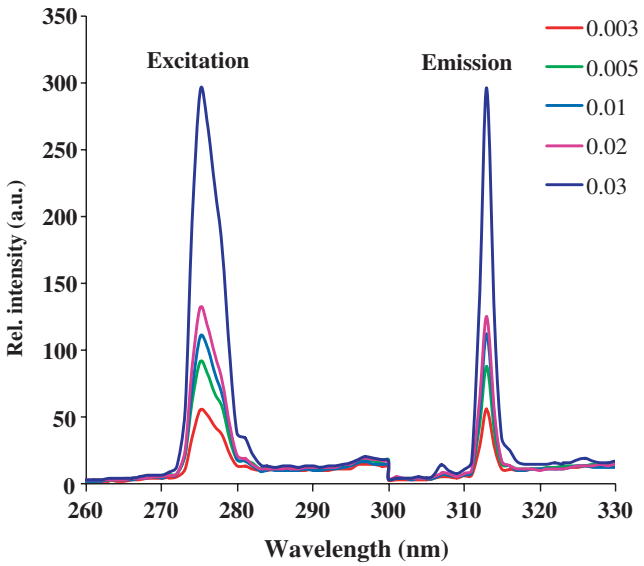

Figure 5. PL excitation (monitored at 313 nm) and emission (monitored at 276 nm) spectra of $LiSr_{4-x}(BO_3)_3:_xGd^{3+}$ synthesized by precipitation method.

Figure 6 presents the combined excitation and emission spectra of $LiSr_{4-x-y}(BO_3)_3:_xGd^{3+}$, $_yPr^{3+}$ phosphors. With increasing molar ratio of Pr^{3+} in $LiSr_{4-x-y}(BO_3)_3:_xGd^{3+}$, $_yPr^{3+}$ and the concentration of Gd^{3+} remaining constant at 0.03 mol, we note the following change in the spectrum: the excitation peak shifted towards the shorter wavelength side. The photoluminescence spectra of $LiSr_4(BO_3)_3$ doped with Gd^{3+}, Pr^{3+} show that emission is in the form of a narrow-band UVB at 313 nm corresponding to $^6P_J \rightarrow {}^8S_{7/2}$ transition upon excitation with 245 nm. The broad excitation spectrum has a maximum located at 245 nm, due to overlap of $4f^15d^1$ interconfigurational transition of Pr^{3+} and $^8S_{7/2} \rightarrow {}^6D_J$ transition of Gd^{3+} and a weak intense band at about 276 nm corresponding to $^8S_{7/2} \rightarrow {}^4I_J$ of Gd^{3+}. From this it can be concluded that most of the excitation energy is absorbed by Pr^{3+} ions.

We also investigated the photoluminescence spectra of $LiSr_4(BO_3)_3$ with different doping concentrations of Pr^{3+} at the constant Gd^{3+} concentration of 0.03 mol. The emission intensity of $LiSr_4(BO_3)_3:Gd^{3+}$–Pr^{3+} increases with increasing Pr^{3+} doping concentration and reaches a maximum at 0.01 mol. When the doping concentration of Pr^{3+} ion in $LiSr_4(BO_3)_3:Gd^{3+}$–Pr^{3+} exceeds 0.01 mol, the emission intensity of the synthesized phosphor decreases due to the concentration quenching as shown in figure 7.

To calculate the critical distance of $LiSr_4(BO_3)_3:Gd^{3+}$, Pr^{3+} the crystallographic data were the same as mentioned

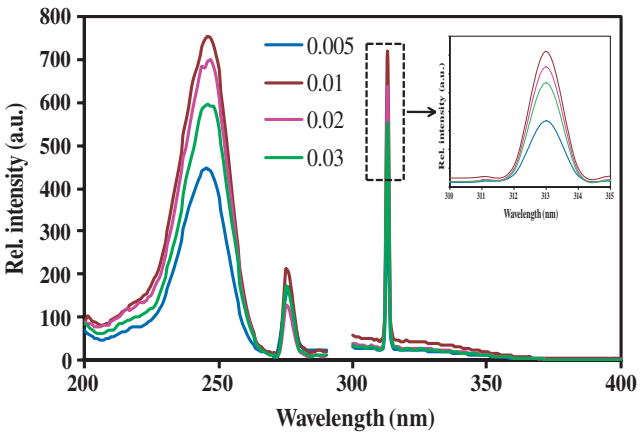

Figure 6. PL excitation and emission spectra of $LiSr_{4-x-y}(BO_3)_3:_xGd^{3+}$, $_yPr^{3+}$ synthesized by solid-state diffusion method.

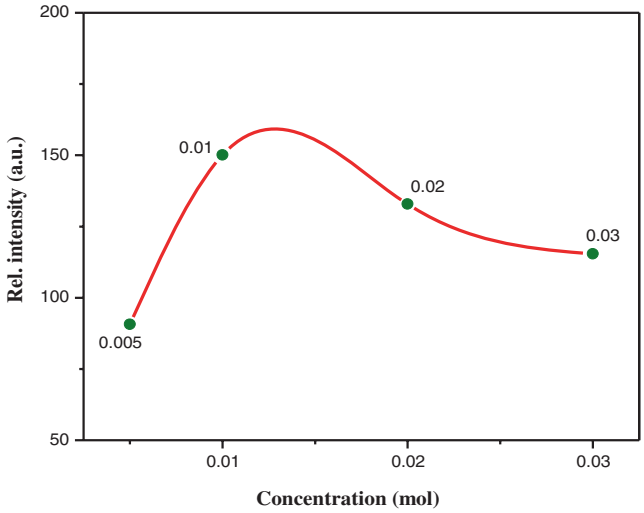

Figure 7. Plot of relative intensity *vs.* concentration of Pr^{3+}.

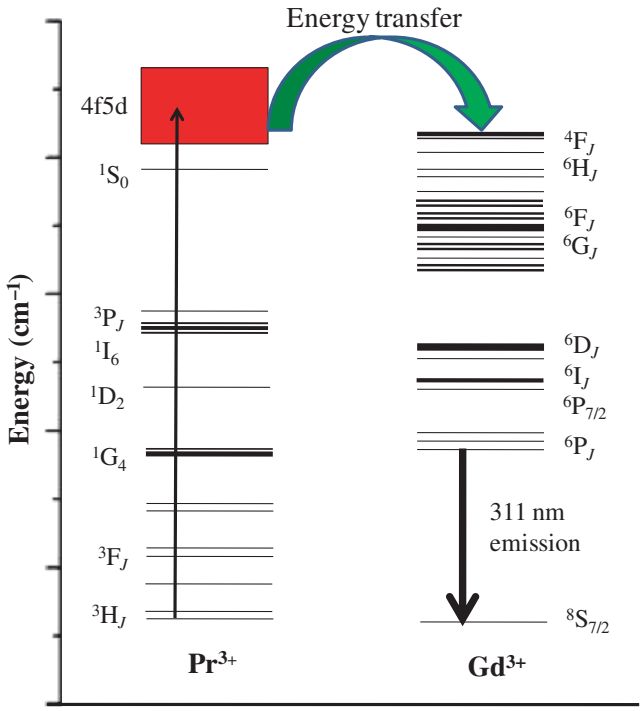

Figure 8. Energy transfer mechanism of Pr^{3+} to Gd^{3+}.

above except that the value of χ_c was changed, i.e., χ_c is about 0.04 (the sum of Gd^{3+} concentration of 0.03 mol and the Pr^{3+} concentration of 0.01 mol). The critical distance R_C of $LiSr_4(BO_3)_3:Pr^{3+}$ phosphor is calculated to be about 21.52 Å.

We observed that the emission is in the form of a narrow band at 313 nm, which corresponds to $^6P_J \rightarrow {}^8S_{7/2}$ transition of Gd^{3+}; no traces of Pr^{3+} emission were observed in the emission spectra and the narrow-band emission intensity of phosphor increases with addition of Pr^{3+} ions, which confirm that the energy is effectively transferred from $Pr^{3+} \rightarrow Gd^{3+}$ ions in $LiSr_{4-x-y}Gd_xPr_y(BO_3)_3$ phosphors. The mechanism is schematically described in figure 8. The very-low-intensity broadness observed in the range 300–350 nm may be due to Pr^{3+} ions emission. From this it can be concluded that most of the excitation energy is absorbed by Pr^{3+} ions and transferred to Gd^{3+} ion.

5. Conclusions

In this work $LiSr_{4-x}Pr_x(BO_3)_3$, $LiSr_{4-x}Gd_x(BO_3)_3$ and $LiSr_{4-x-y}Gd_xPr_y(BO_3)_3$ phosphors have been successfully synthesized using a modified solid-state diffusion method.

The photoluminescence spectra of $LiSr_{4-x}Pr_x(BO_3)_3:Pr^{3+}$ reveal that the broad emission spectra of phosphor belong to UV region, i.e., 260–370 nm which has good overlap with the region in which the excitation of Gd^{3+} ion is observed. Because of this reason we considered that Pr^{3+} is a good sensitizer in case of $LiSr_4(BO_3)_3$ phosphor.

The room-temperature photoluminescence spectra of synthesized $LiSr_{4-x}Gd_x(BO_3)_3$ phosphors show emissions at wavelengths 313 nm under 276 nm excitation radiation. These emission wavelengths lie in a narrow-band UVB region of electromagnetic spectrum. Optimum concentration for 313 nm emission was found to be about 0.03 mol.

The emission spectra of $LiSr_{4-x-y}Gd_xPr_y(BO_3)_3$ phosphors are also in the narrow-band UVB region under the excitation of 245 nm. The broadband excitation spectra show very good overlap with the Hg 253.7 nm line. The photoluminescence spectra of $LiSr_4(BO_3)_3$ with different doping concentrations Pr^{3+} and keeping the concentration of Gd^{3+} constant at 0.03 mol have also been studied. The emission intensity of $LiSr_4(BO_3)_3:Gd^{3+}$–Pr^{3+} phosphors increases with increasing Pr^{3+} doping concentration and reaches a maximum at 0.01 mol. When the doping concentration of Pr^{3+} ion in $LiSr_4(BO_3)_3:Gd^{3+}$ exceeds 0.01 mol, the emission intensity of the synthesized phosphor decreases. Efficient energy transfer from $Pr^{3+} \rightarrow Gd^{3+}$ ions in $LiSr_{4-x-y}Gd_xPr_y(BO_3)_3$ phosphor was observed. As a result, $LiSr_{4-x-y}Gd_xPr_y(BO_3)_3$ phosphor is a good candidate as a narrow-band UVB-emitting phosphor for phototherapy applications. The critical energy transfer distance for $LiSr_{4-x}Pr_x(BO_3)_3$, $LiSr_{4-x}Gd_x(BO_3)_3$ and $LiSr_{4-x-y}(BO_3)_3:{}_xGd^{3+}$, ${}_yPr^{3+}$ was found to be 34.17, 23.69 and 21.52 Å, respectively.

Acknowledgements

AOC is thankful to the Chairman, FIST-DST Project, SGBA University, Amravati (MH) 444602, India, for providing XRD facility for this work. The author also thanks Dr S B Kondawar, Department of Physics, RTM University, Nagpur (MH) 440013, India, for providing access to SEM.

References

[1] Weichenthal M and Schwarz T 2005 *Photodermatol. Photoimmunol. Photomed.* **21** 260

[2] Weelden H V, Faille H B D L, Young E and Leun J C V 1988 *Br. J. Dermatol.* **11** 119

[3] Johnson B, Green C, Lakshmipathi T and Ferguson J 1988 *Light in biology and medicine* (NY, London: Plenum Press) p 173

[4] Sonekar R, Omanwar S, Moharil S, Dhopte S, Muthal P and Kondawar V 2007 *Opt. Mater.* **30** 622

[5] Ferguson J 1999 *Arch. Dermatol.* **135** 589

[6] Zhang Y, Chen X, Liang J, Cao Y and Xu T 2001 *J. Alloys Compd.* **198** 315

[7] Guo C, Ding X, Seo H J, Ren Z and Bai J 2011 *J. Alloys Compd.* **509** 4871

[8] Zhang X, Lang H and Seo H 2011 *J. Fluoresc.* **21** 1111

[9] Zhang Z W 2013 *Ceram. Int.* **39** 1723

[10] Yu H 2012 *J. Lumin.* **132** 2553

[11] Wang Q 2012 *J. Lumin.* **132** 434

[12] Palan C, Bajaj N and Omanwar S 2016 *Mater. Res. Bull.* **76** 216

[13] Palan C, Bajaj N, Soni A and Omanwar S 2016 *J. Lumin.* **176** 106

[14] Bajaj N, Palan C, Koparkar K, Kulkarni M and Omanwar S 2016 *J. Lumin.* **175** 9

[15] Shannon R 1976 *Acta Crystallogr. A* **32** 751

[16] Blasse G 1969 *Philips. Res. Rep.* **24** 131